APPENDIX A

Mathematical calculations underlying the normalization procedure

Let (X_i, Y_i) be the pair of values responding the micrometer reading and force reading respectively characterizing each step in the normalization procedure. Y_0 is the force reading at the start position of the normalization procedure where the wires are just separated and the force reading is approximately zero. Then given that tension on the vessel is equal to force divided by wall length, the wall tension at the i^{th} micrometer reading is calculated by: $T_i = Y_i - Y_o / 2\delta \cdot |a_1 - a_2|$, where is the microscope eyepiece reticule calibration factor in mm per division and a_1 and a_2 are the vessel end points when measuring the length of the mounted vessel segment.

The internal circumference of the mounted vessel at the i^{th} reading is calculated by: $IC_i = IC_o + 2(X_i - X_0)$, where IC_0 is the internal circumference of the mounted vessel when the wires are just separated and is given by: $IC_o = (2+\pi) \cdot d$, where d is the wire diameter.

Using the Laplace relation, the effective pressure P_i is calculated for each pair of readings by: $P_i = T_i / (IC_i / 2\pi)$. The effective pressure is an estimate of the internal pressure, which is necessary to extend the vessel to the measured internal circumference.

The stepwise distension is continued until the calculated effective pressure exceeds the target transmural pressure (Figure 45A). For rat mesenteric arteries the target transmural pressure is normally 100 mm Hg (13.3 kPa), but the value needs to be optimized for individual types of tissue preparations. An exponential curve is fitted to the internal circumference pressure data as illustrated in Figure 45B. The isobar corresponding to 100 mmHg is used to calculate the IC_{100} value from the point of interception between the function of the exponential curve and the function of the 100 mmHg isobar: $T_{100} = 100 \cdot (IC / 2\pi)$.

The normalized internal circumference IC_1 is calculated by: $IC_1 = k \cdot IC_{100}$, where the factor k is for rat mesenteric arteries 0.9, but has to be optimized for each particular tissue preparation.

The micrometer reading X_1, at which the normalized internal circumference is attained is calculated by: $X_1 = X_0 + (IC_1 - IC_0 / 2)$. The normalized internal diameter is calculated by: $l_1 = IC1 / \pi$. (User manual: Dual wire myograph system model 410A, version 2.00, 2003)

(A)

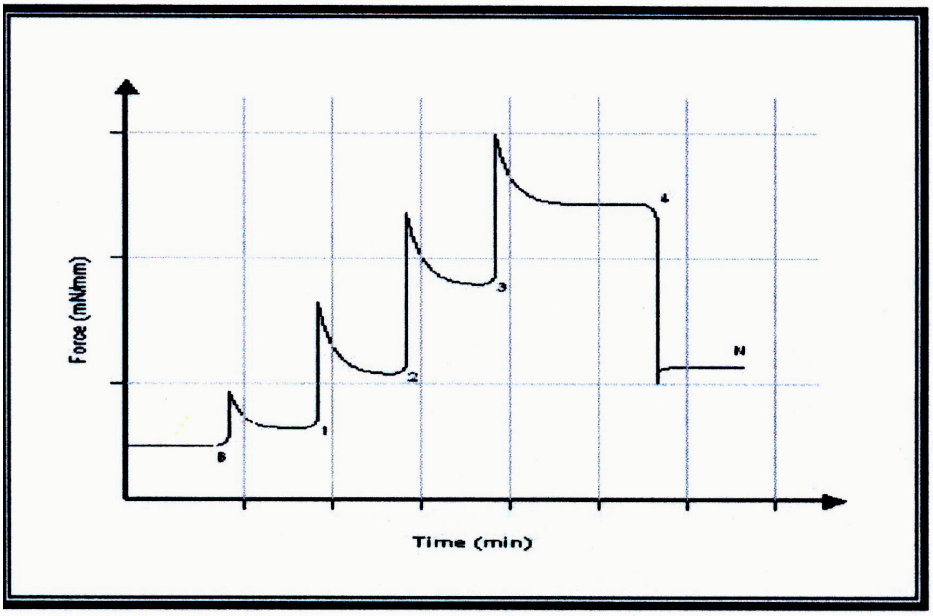

(B)

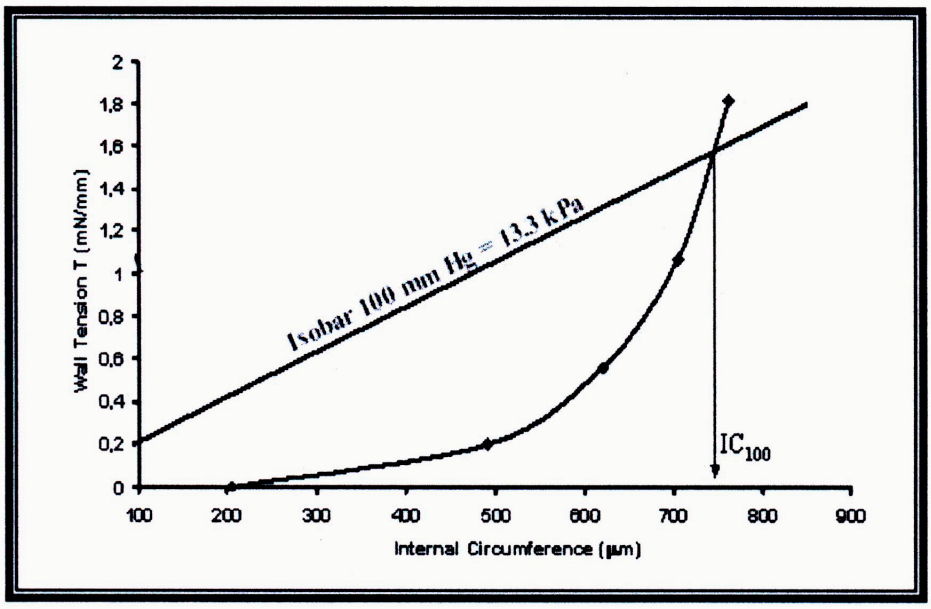

Figure 44 Illustration showing the stepwise normalisation procedure (A) and the exponential curve fitting and calculation of IC_{100} (B).

APPENDIX B

Structural determination of isolated compounds from *R. siamensis* extract

Results and discussion

11 compounds were isolated from the *Randia siamensis* extract. The chemical structures were elucidated by Prof. Hostettmann and his colleges, University of Geneva, Switzerland using MS, ^{1}H and ^{13}C NMR analysis as in the following details.

Kaempferol-3-O-β-xylose (1-2)- β-galactoside (**1**): Yellow amorphous powder. For MS, ^{1}H and ^{13}C NMR data, see Markham and Mabry (1975).

Kaempferol-3-O-β-galactoside (**2**): Yellow amorphous powder. For MS, ^{1}H and ^{13}C NMR data, see Markham and Mabry (1975).

Pseudoginsenoside-RP$_1$ (**3**): white amorphous powder. For MS, ^{1}H and ^{13}C NMR data, see Inada et al. (1987).

Pseudoginsenoside-RT$_1$ methyl ester (**4**): white amorphous powder. For MS, ^{1}H and ^{13}C NMR data, see Sakai et al. (1994).

Tyramine (**5**): white amorphous powder. For MS, ^{1}H and ^{13}C NMR data, see Graziano et al. (1971).

Pseudoginsenoside-RT$_1$ (**6**): white amorphous powder. For MS, ^{1}H and ^{13}C NMR data, see Ida et al. (1994).

Pseudoginsenosides-RT$_5$ (**7**): White amorphous powder. HRESIMS: *m/*z 1087.3435 (calcd for $C_{53}H_{84}O_{23}$ [M-H]□, calc. 1087.3435). ESI-MS (negative mode): *m/*z 1087.3 [M-H]□□, 942 [M-rhamnose]□□, 809 [M-rhamnose-arabinose]□□. ^{1}H NMR (DMSO-d_6, 500 MHz): □ see table 2. ^{13}C NMR (DMSO-d_6, 125 MHz): □ see table 3.

Pseudoginsenosides-RT$_3$ (8): White amorphous powder. HRESIMS: *m/*z 942 (calcd for $C_{47}H_{74}O_{19}$ [M-H]□□, calc. 942). ESI-MS (negative mode): *m/*z 942 [M-H]□□, 809 [M-

arabinose]□□, 647 [M- arabinose-glucose]□□. ^{1}H NMR (DMSO-d_6, 500 MHz): □ see table 2. ^{13}C NMR (DMSO-d_6, 125 MHz): □ see table 3.

5-O-[Z] caffeoylquinic acid (9): For MS, ^{1}H and ^{13}C NMR data, see King et al. (1957).

Pseudoginsenosides-RT$_4$ (10): White amorphous powder. HRESIMS: *m/*z 1119 (calcd for $C_{53}H_{84}O_{23}$ [M-H]□□, calc. 1119). ESI-MS (negative mode): *m/*z 1119 [M-H]□□, 957 [M-glucose]□□.^{1}H NMR (DMSO-d_6, 500 MHz): □ see table 2. ^{13}C NMR (DMSO-d_6, 125 MHz): □ see table 3

Pseudoginsenosides-RT$_2$ (11): White amorphous powder. HRESIMS: *m/*z 986 (calcd for $C_{53}H_{84}O_{23}$ [M-H]□□, calc. 986). ESI-MS (negative mode): *m/*z 986 [M-H]□□, 972 [M-CH_3]□□, 811 [M-glucose]□□. ^{1}H NMR (DMSO-d_6, 500 MHz): □ see table 2. ^{13}C NMR (DMSO-d_6, 125 MHz): □ see table 3.

Table 2 Selected ^{1}H NMR (value) data of compound **7**,**8**,**10** and **11.**

Position	**7 (RT_5)**	**8 (RT_3)**	**10 (RT_4)**	**11 (RT_2)**
3	2.98, m	3.08, m	3.06, m	3.06, m
12	5.15, br s	5.17, br s	5.15, br s	5.16, br s
23	1.04, s	0.97, s	0.97, s	0.96, s
24	0.72, s	0.75, s	0.75, s	0.66, s
25	0.74, s	0.74, s	0.74, s	0.74, s
26	0.84 , s	0.86, s	0.86, s	0.8, s
27	0.98, s	1.09, s	1.09, s	1.09, s
29	3.1-3.46, m	3.0.-3.45, m	0.9, m	3.01-3.5, m
30	0.92, s	0.91, s	0.92, s	0.9, s
	glucose at C-29	**glucose at C-29**	**glucuronic acid at C-3**	**glucose at C-29**
1'	4.06 (d, *J*=7.81 Hz)	4.09 (d, *J*=7.32 Hz)	4.43 (d, *J*=6.84 Hz)	4.07 (d, *J*=6.84 Hz)
2'	2.95	2.97	3.3	2.96
3'	3.16	3.15	3.16	3.18
4'	3.08	3.06	3.40	3.05
5'	3.1	3.1	3.67	3.16
6'	3.42-3.64	3.45-3.68	-	3.41-3.58
	glucuronic acid at C-3	**glucuronic acid at C-3**	**glucose**	**glucuronic acid at C-3**
1''	4.14 (d, *J*=6.84 Hz)	4.41 (d, *J*=6.84 Hz)	4.07 (d, *J*=6.34 Hz)	4.41 (d, *J*=6.34 Hz)
2''	3.34	3.3	2.98	3.3
3''	3.41	3.16	3.14	3.4
4''	3.65	3.41	3.06	3.68
5''	3.92	3.67	3.1	3.63

6’’	-	-	3.40-3.66	-
-OCH_3				3.68
	arabinose	**arabinose**	**glucose**	**glucose**
	4.76 (d, *J*=6.34	4.40 (d, *J*=6.84	4.71 (d, *J*=6.84	4.31 (d, *J*=6.34
1’’’	Hz)	Hz)	Hz)	Hz)
2’’’	3.16	3.13	3.39	3.23
3’’’	3.22	3.42	3.24	3.19
4’’’	3.3	3.3	3.38	3.4
5’’’	2.94-3.65	3.02-3.68	3.06	3.15
6’’’			3.38-3.66	3.46-3.58
	rhaminose		**glucose**	
	4.99 (br		4.41 (d, *J*=6.84	
1’’’’	singulet)		Hz)	
2’’’’	3.65		2.96	
3’’’’	3.14		3.28	
4’’’’	3.72		3.03	
5’’’’	3.77		3.1	
6’’’’	1.01		3.42-3.68	

Table 3 Selected ^{13}C NMR (value) data of compound **7**,**8**,**10** and **11**.

Position	**7 (RT_5)**	**8 (RT_3)**	**10 (RT_4)**	**11 (RT_2)**
3	89.0	90.0	90	88.3
12	123.6	123.6	123.6	121.6
24	16.3	15.9	15.9	16.8
25	15.3	17.8	17.8	15.1
26	18.1	17.0	17	22.0
27	27.8	26.4	26.4	25.4
28	178.4	178.6	178.4	178.5
29	79.9	80.0	32.7	79.8
30	19.5	20.1	23.3	19.1
	Gluc at C-29	**Gluc at C-29**	**Glucur acid at C-3**	**Gluc at C-29**
1'	103.6	104	105	104.1
2'	73.02	74	82	73.9
3'	78.4	77.2	77	76.6
4'	71.1	71	73.5	71
5'	78.5	77.5	76.8	77.7
6'	61.1	62	170.1	61.09
	Glucur acid at C-3	**Glucur acid at C-3**	**Glucose**	**Glucur acid at C-3**
1''	103.9	105	104	104.7
2''	77.6	82	75	76.8
3''	76.8	76.4	77.5	87.7
4''	80.1	70.9	70.8	72.3
5''	75.6	75.6	75.8	76
6''	170.1	170	66.6	169.9
-OCH_3				53

	arabinose	**arabinose**	**glucose**	**glucose**
1’’’	100.6	103	102	103.4
2’’’	76.5	77	83.7	73.9
3’’’	75.4	75.6	77.4	76.6
4’’’	77.8	70.5	70.1	71
5’’’	65.6	66.5	78.2	77.7
6’’’			61.1	61.09
	rhaminose		**glucose**	
1’’’’	100.2		105	
2’’’’	70.6		76.2	
3’’’’	68		78.4	
4’’’’	74.2		71.1	
5’’’’	70.0		78.5	
6’’’’	18.1		61.5	

Compounds **1**-**6** and **9** were easily identified from chemical and spectroscopic data and by comparison with literature data as kaempferol-3-O-□-xylose (1-2)-□-gylactoside (**1**), kaempferol-3-O-□-galactoside (**2**), pseudoginsenoside-RP_1 (**3**), pseudoginsenoside-RT_1 methyl ester (**4**), tyramine (**5**), pseudoginsenoside-RT_1 (**6**) and 5-O-[*Z*] caffeoylquinic acid (**9**).

Saponin **7** was obtained as a white powder. The presence of four sugars molecules was indicated by its ^{1}H NMR spectrum, which showed signals for four anomeric protons at □ 4.06, 4.14, 4.76 and 4.96. Acid hydrolysis of **7** with HCL 2N resulted in an aglycon identified by ^{1}H and ^{13}C NMR and by MS as Olean-12-en-28-oic acid, 3,29-dihydroxy (Mesembryanthemoidigenic acid) while sugar analysis by GC-MS after sylilation revealed the presence of glucose, rhaminose, arabinose and glucuronic acid. HRESIMS showed a protoaned molecular ion at *m/z* 1087.3435 $[M-H]^{+}$, consisted with a protoaned molecular formula $C_{53}H_{84}O_{23}$. These data are in agreement with an aglycone substituted by four sugars. Moreover, the ESIMS analysis showed the fragments ions at *m/z* 942 $[M\text{-Rhaminose}]^{+}$ and 809 $[M\text{-rham-arabinose}]^{+}$ indicating the sequence of sugars. The linkage of sugars unit was obtained by the carefully

analysis of 2D NMR spectra and by selective TOCSY 1D analysis. In the HMBC spectrum the correlations between the anomeric protons at □ 4.14 and 4.06 and the carbons at □ 89.0 and 80.0 respectively, indicated the attachment of two sugar units in positions C-3 and C-29. On the basis of HMBC, HSQC, ^{1}H-^{1}H COSY, and TOCSY spectra, all proton and carbon signals of these sugars were assigned. The HMBC spectrum data elucidate the sugar sequence as rhaminose-(1□4)-arabinopyranosyl-(1□4)-glucuronic acid as supported by HMBC cross-pecks of H-1 (□ 4.99) rhaminose with C-4 (□ 77.8) arabinose, H-1 arabinose (□ 4.76) with C-4 (□ 80.9) glucoronic acid. The 2D NMR analysis allowed to the identification of glucose in position C-29, and a glucuronic acid in position C-3. Compound **7** was identified as Olean-12-en-28-oic acid-3-O-□-glucuronic acid-(4□1)-[□ □-arabinopyranosyl]-(4□1)-[□ □-Rhamnopyranosil]-29-O-□-glucopyranoside named **pseudoginsenoside-RT$_5$**.

Saponin **8** presented an molecular ion at *m/z* 942.3435 $[M-H]^+$ in the HRESIMS analysis, which consist in the molecular formula at $C_{47}H_{74}O_{19}$. The ^{1}H NMR spectrum showed the presence of three signals at □ 4.0, 4.09 and 4.41, correlated with those of three carbons at □ 103, 104 and 105 by an HMQC experiment and was diagnostic for the presence of three sugars. The GC-MS analysis after acid hydrolysis of **8** afforded aglycone, glucose, arabinose and glucuronic acid. As for saponin **7**, the on the basis of 2D NMR spectra, all proton and carbon signals of these sugars were assigned. The HMBC spectrum data elucidate the sugar sequence as arabinopyranosyl-(1□2)-glucuronic acid. The correlations observed in the HMBC spectrum between □ 4.41 and □ 90.0 indicated the presence of a glucuronic acid in position C-3 while the glucose correlations between □ 4.09 and □ 80.0 indicated the presence of a glucose in position C-3. Compound **8** was identified as Olean-12-en-28-oic acid-3-O-□-glucuronic acid-(4□1)-[□-arabinopyranosyl]-29-O-□-glucopyranoside named **pseudoginsenoside-RT$_3$**.

Saponin **10** presented an molecular ion at *m/z* 1119.2 $[M-H]^+$ in the HRESIMS analysis, which consist in the molecular formula at $C_{54}H_{86}O_{24}$. The GC-MS analysis after acid hydrolysis of **10** afforded aglycone, glucose and glucuronic acid. On the basis of HMBC, HSQC, ^{1}H-^{1}H COSY, and TOCSY spectra, all proton and carbon signals of these sugars were assigned. The HMBC spectrum data elucidate the sugar sequence as glucopyranosyl(1□2)-glucopyranosyl-(1□6)-glucopyranosyl-(1□2)-glucuronic acid. The attachment of the sugar chain at carbon C-3 was obtained by the HMBC spectrum. Compound **10** was identified as

Olean-12-en-28-oic acid, 3-O-□-glucuronic acid-(1□2)-O-[□-glucopyranosyl]-(1□6)-[□□-glucopyranosyl]-(1□2)-[□□-glucopyranoside]-(1□2)-[□□-glucopyranoside], named **pseudoginsenoside-RT$_4$**.

Saponin **11** presented an molecular ion at *m/z* 986 $[M-H]^+$ in the HRESIMS analysis, in agreement with the molecular formula at $C_{49}H_{76}O_{20}$. The GC-MS analysis after acid hydrolysis of **11** afforded aglycone and glucose and glucuronic acid. The presence of three sugars molecules was indicated by its ^{1}H NMR spectrum, which showed signals for three anomeric protons at □ 4.08 (1H) and 4.27 (2H) correlated with those of three carbons at □ 103, 104.4 and 104.7 by an HMQC experiment. The presence of methyl ester in the glucuronic acid was obtained by HSQC and HMBC spectra. The ^{1}H NMR spectrum showed the methyl signal appears at □ 3.68 (s, 3H) attached to a carbon in the HSQC spectrum at □ 53.0. The HMBC analysis indicated the correlations between this signal and the carbonyl group at □ 169.9 of the glucuronic acid. On the basis of NMR 2D spectra, all proton and carbon signals of these sugars were assigned. The HMBC spectrum data elucidate the sugar sequence as glucopyranosyl-(1□3)-glucuronic acid. The attachment of the sugar chain at carbon C-3 was obtained by the HMBC spectrum. In the HMBC spectrum the correlations between the anomeric protons at □ 4.27 and 4.08 and the carbons at □ 88.3 and 79.8 respectively, indicated the attachment of the sugar units in positions C-3 and C-29. Compound **11** was identified as Olean-12-en-28-oic acid-3-O-□-glucuronic acid-6-methyl ester-(3□1)-[□□-glucopyranosil], 29-O-□-glucopyranoside named **pseudoginsenoside-RT$_2$**.

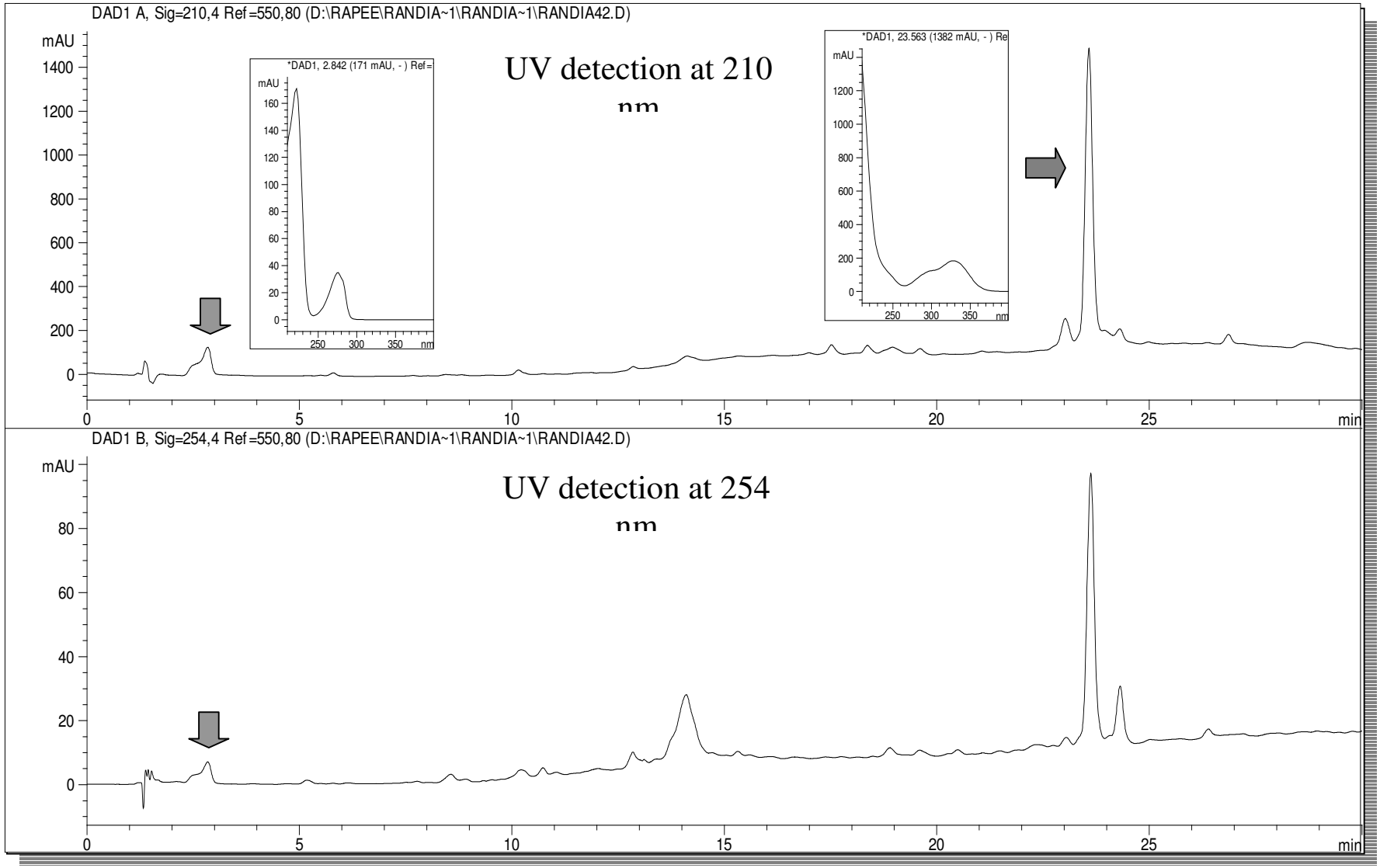

Figure 45 Representative HPLC chromatogram under the UV detection at 210 and 254 nm, and the spectra of two major constituents of

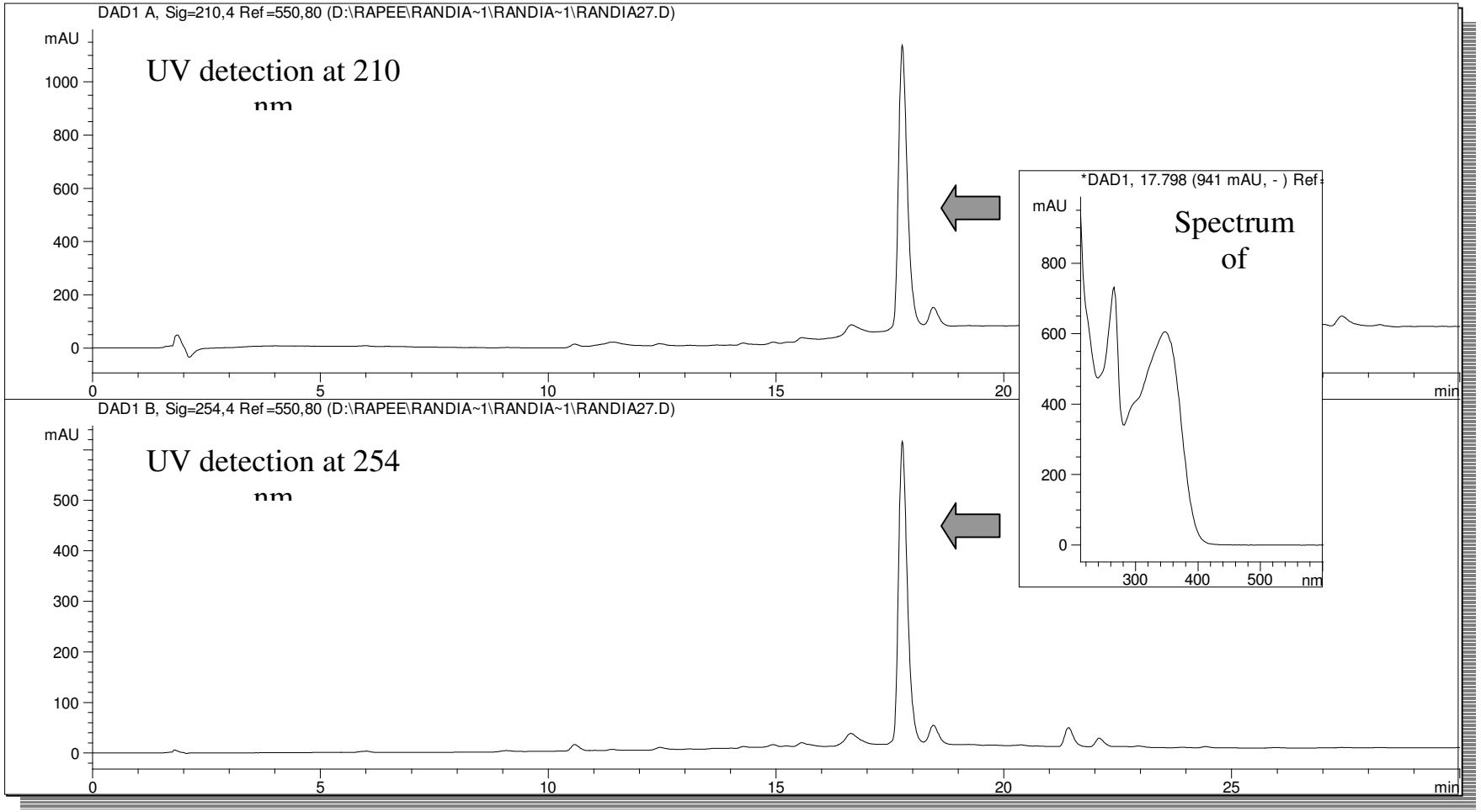

Figure 46 Representative HPLC chromatogram under the UV detection at 210 and 254 nm, and the spectrum of **compound 1,**

Kaempferol-3-O-β-xylose (1-2)- β-galactoside.

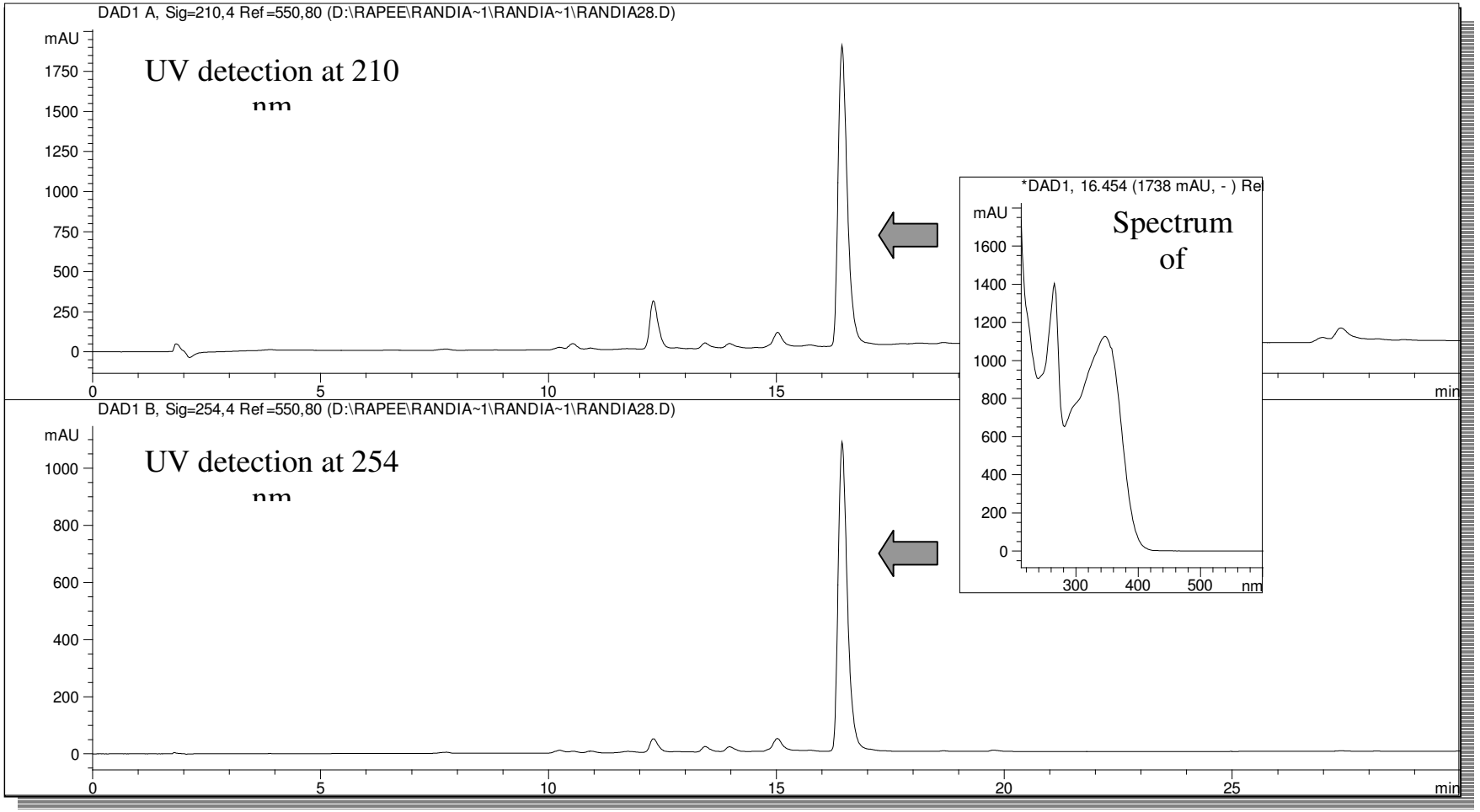

Figure 47 Representative HPLC chromatogram under the UV detection at 210 and 254 nm, and the spectrum of **compound 2,**

Kaempferol-3-O-β-galactoside.

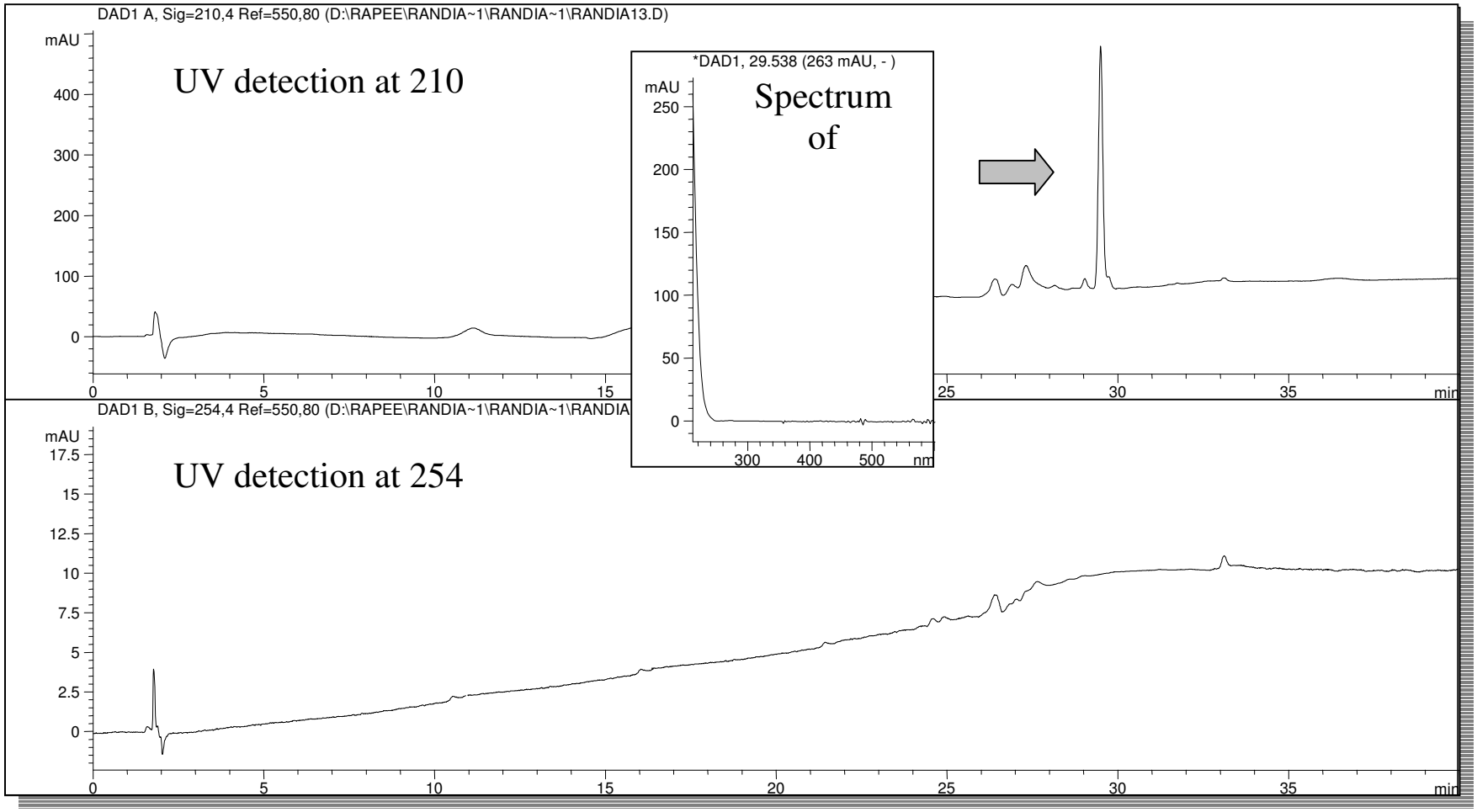

Figure 48 Representative HPLC chromatogram under the UV detection at 210 and 254 nm, and the spectrum of **compound 3,**

Pseudoginsenoside RP

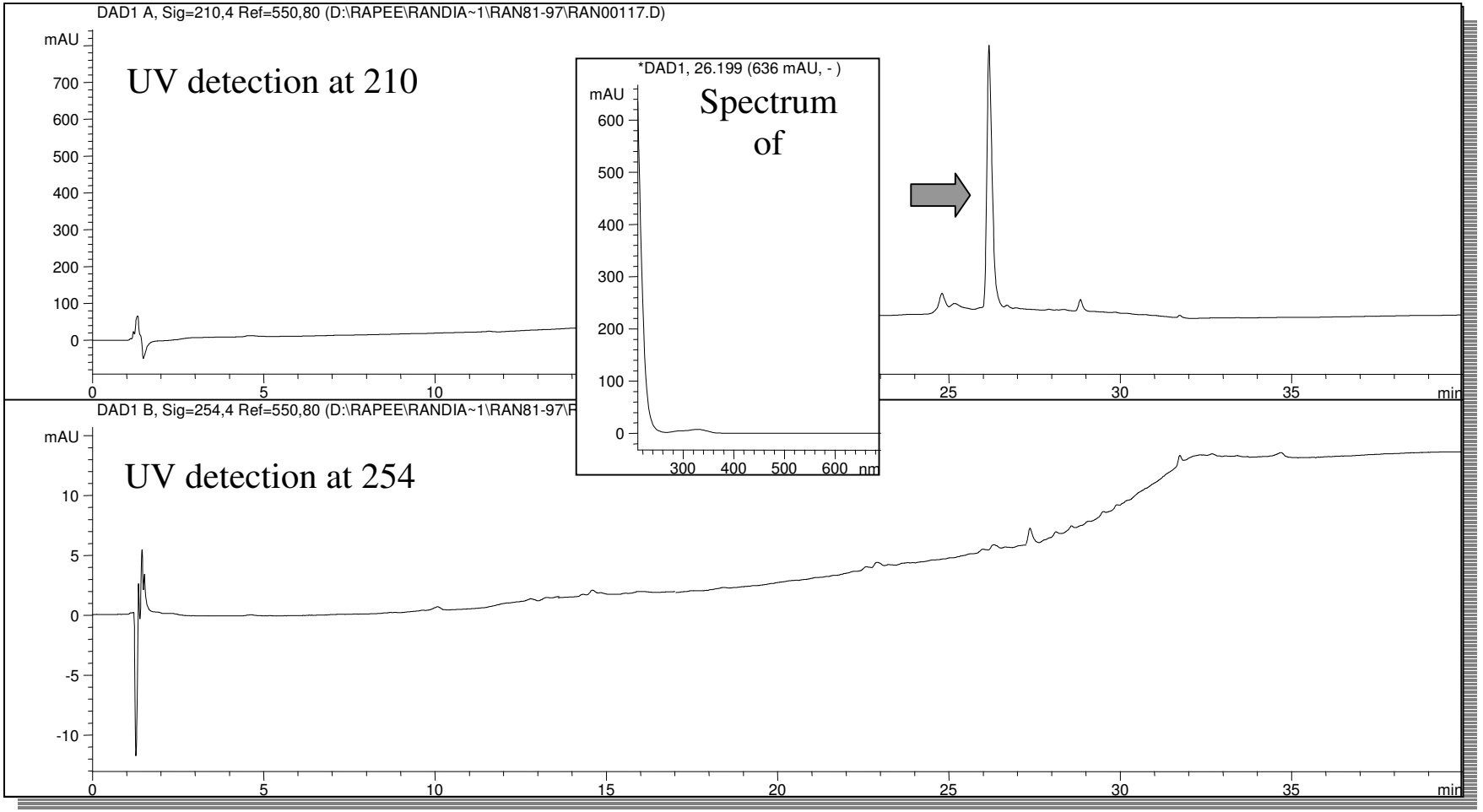

Figure 49 Representative HPLC chromatogram under the UV detection at 210 and 254 nm, and the spectrum of **compound 4,**

Pseudoginsenoside-RT$_1$ methyl ester.

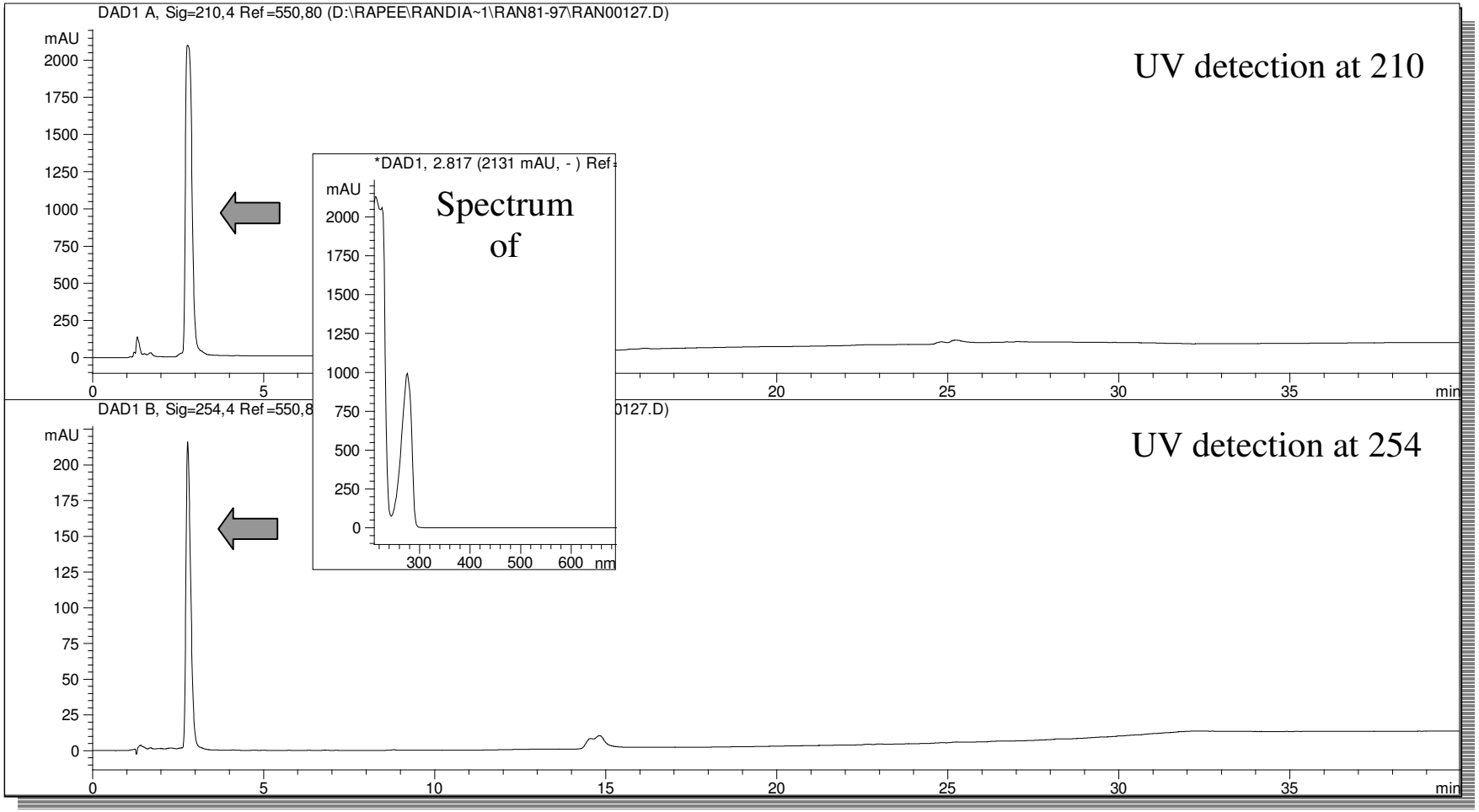

Figure 50 Representative HPLC chromatogram under the UV detection at 210 and 254 nm, and the spectrum of **compound 5, Tyramine**

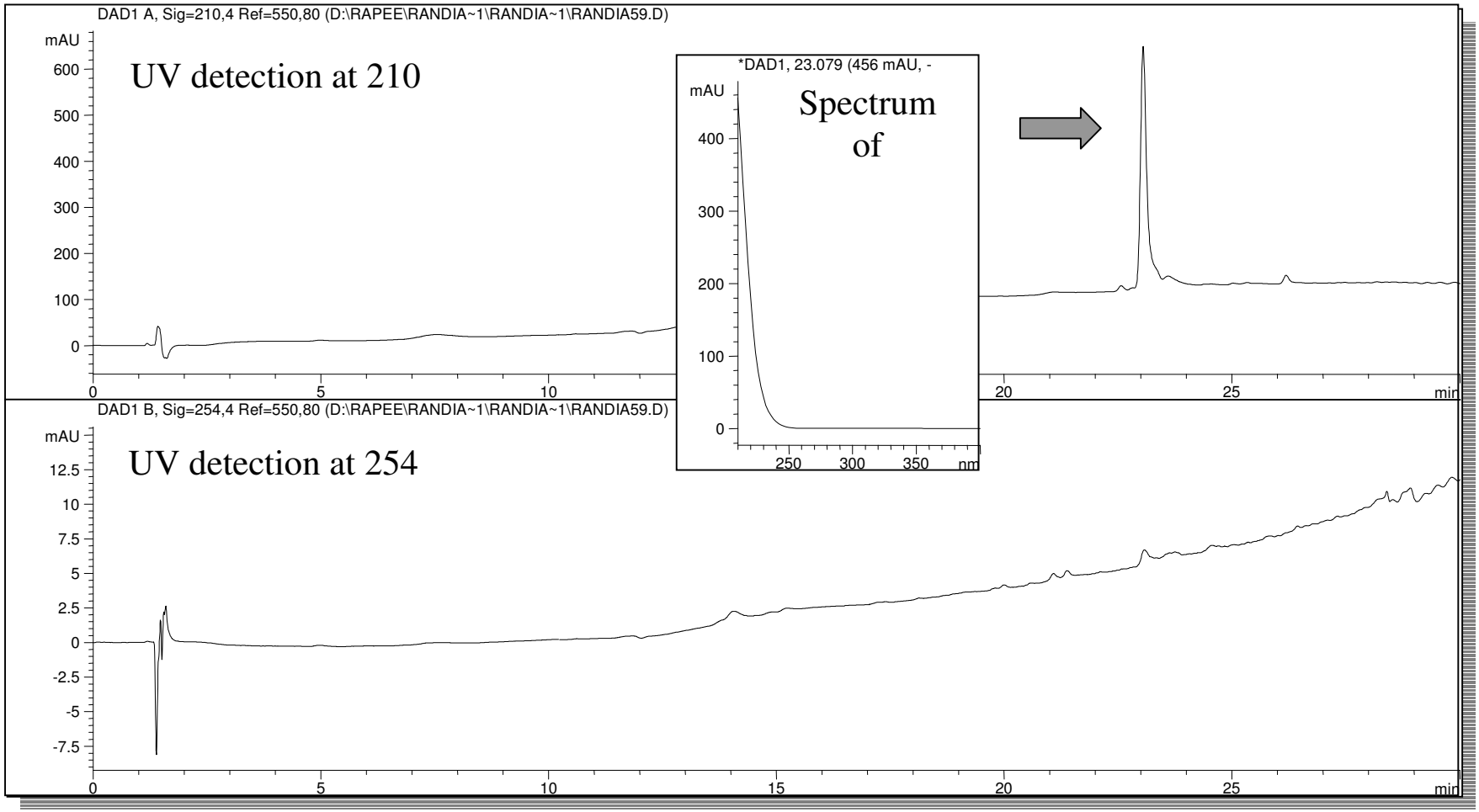

Figure 51 Representative HPLC chromatogram under the UV detection at 210 and 254 nm, and the spectrum of **compound 6,**

Pseudoginsenoside RT

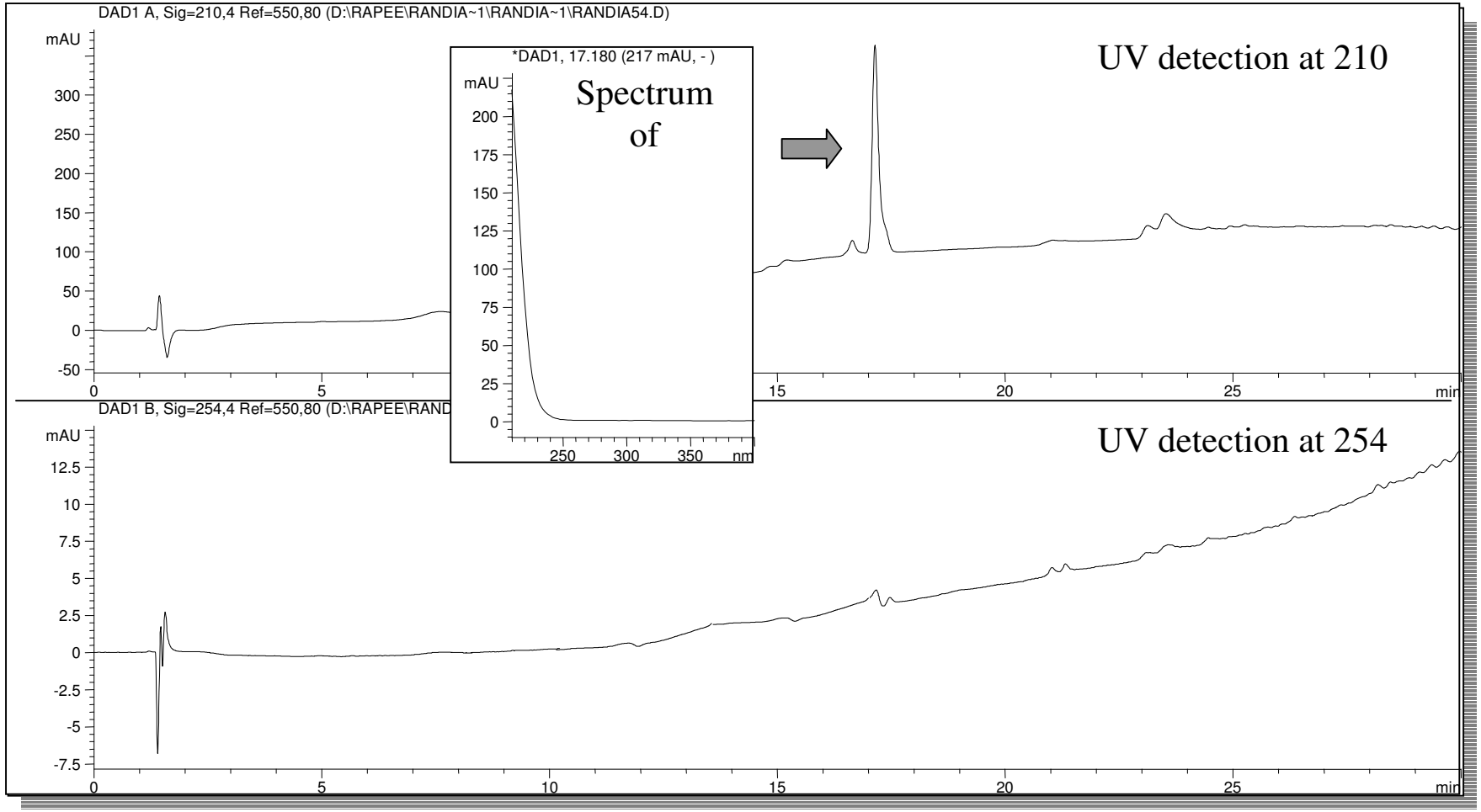

Figure 52 Representative HPLC chromatogram under the UV detection at 210 and 254 nm, and the spectrum of **compound 7,**

Pseudoginsenosides-RT$_5$.

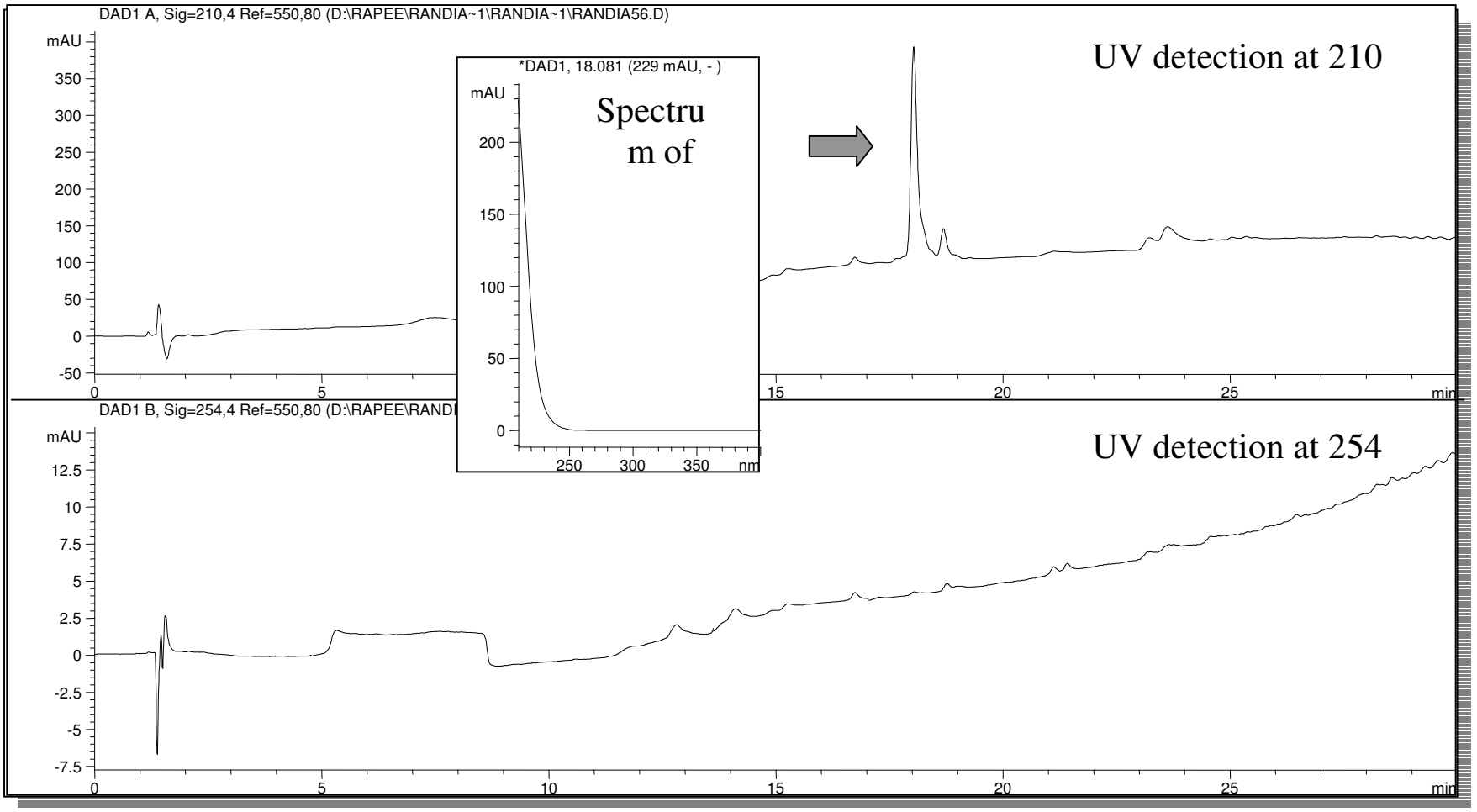

Figure 53 Representative HPLC chromatogram under the UV detection at 210 and 254 nm, and the spectrum of **compound 8,**

Pseudoginsenosides-RT$_3$.

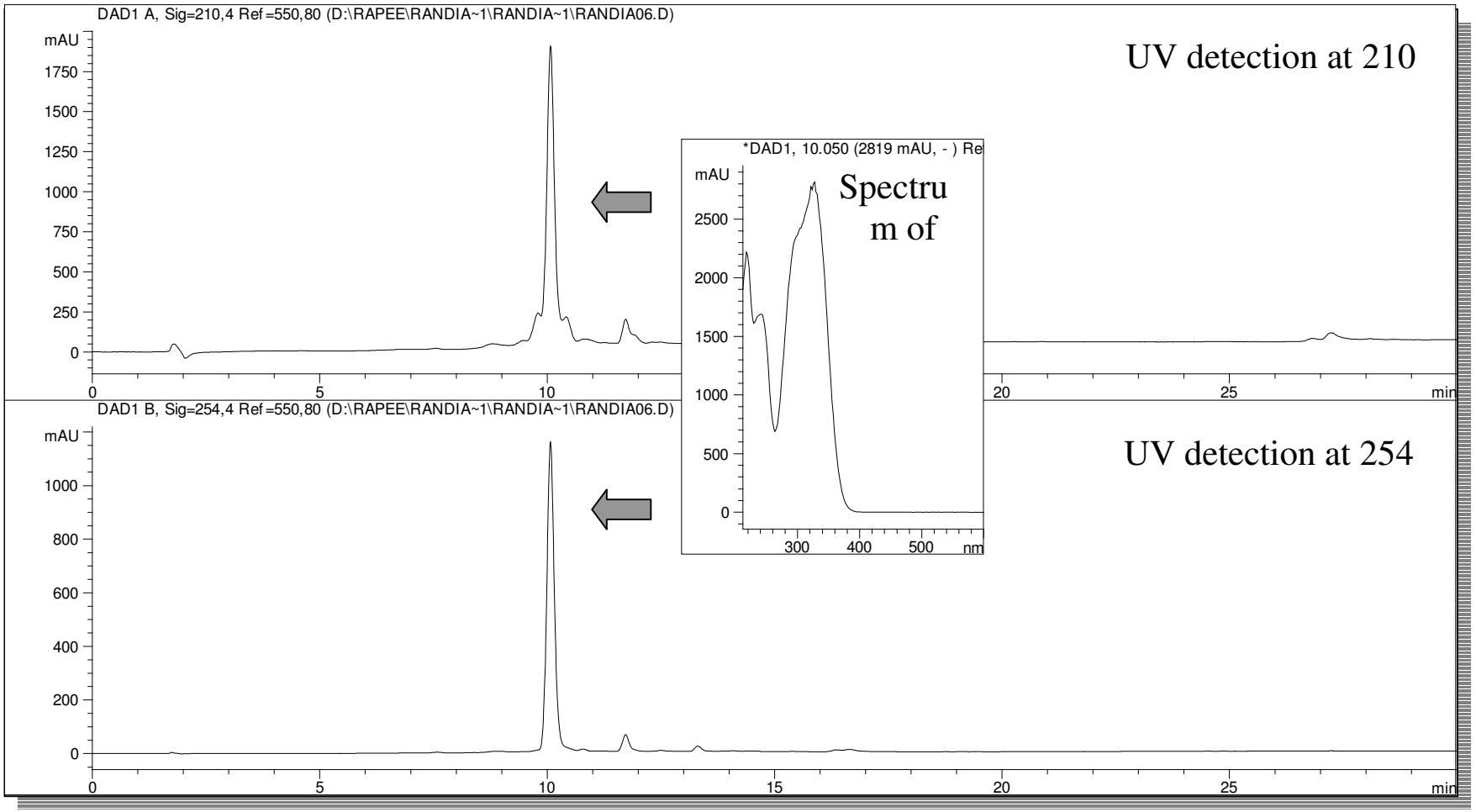

Figure 54 Representative HPLC chromatogram under the UV detection at 210 and 254 nm, and the spectrum of **compound 9,**

5-O-[Z] caffeoylquinic acid.

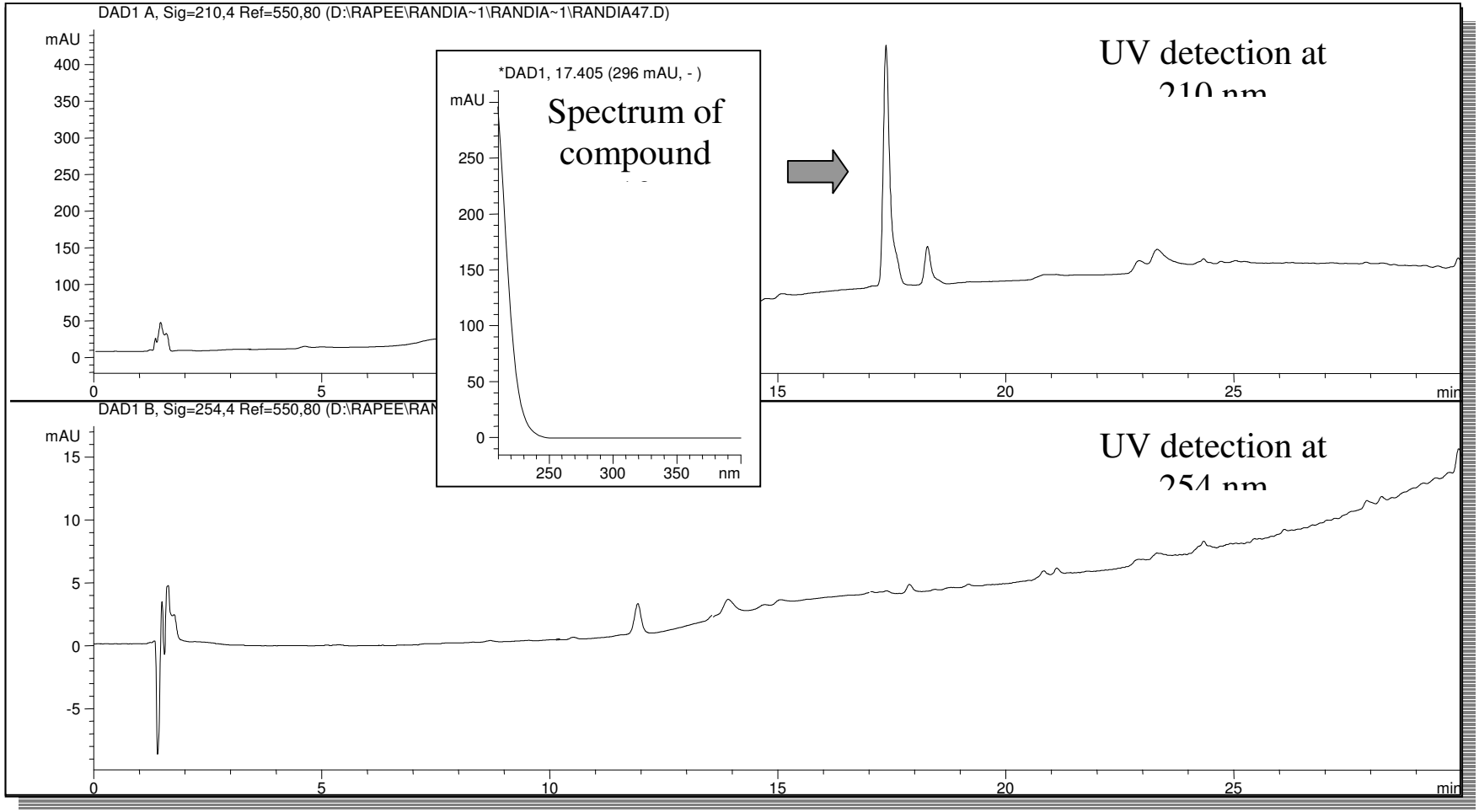

Figure 55 Representative HPLC chromatogram under the UV detection at 210 and 254 nm, and the spectrum of **compound 10,**

Pseudoginsenosides-RT$_4$.

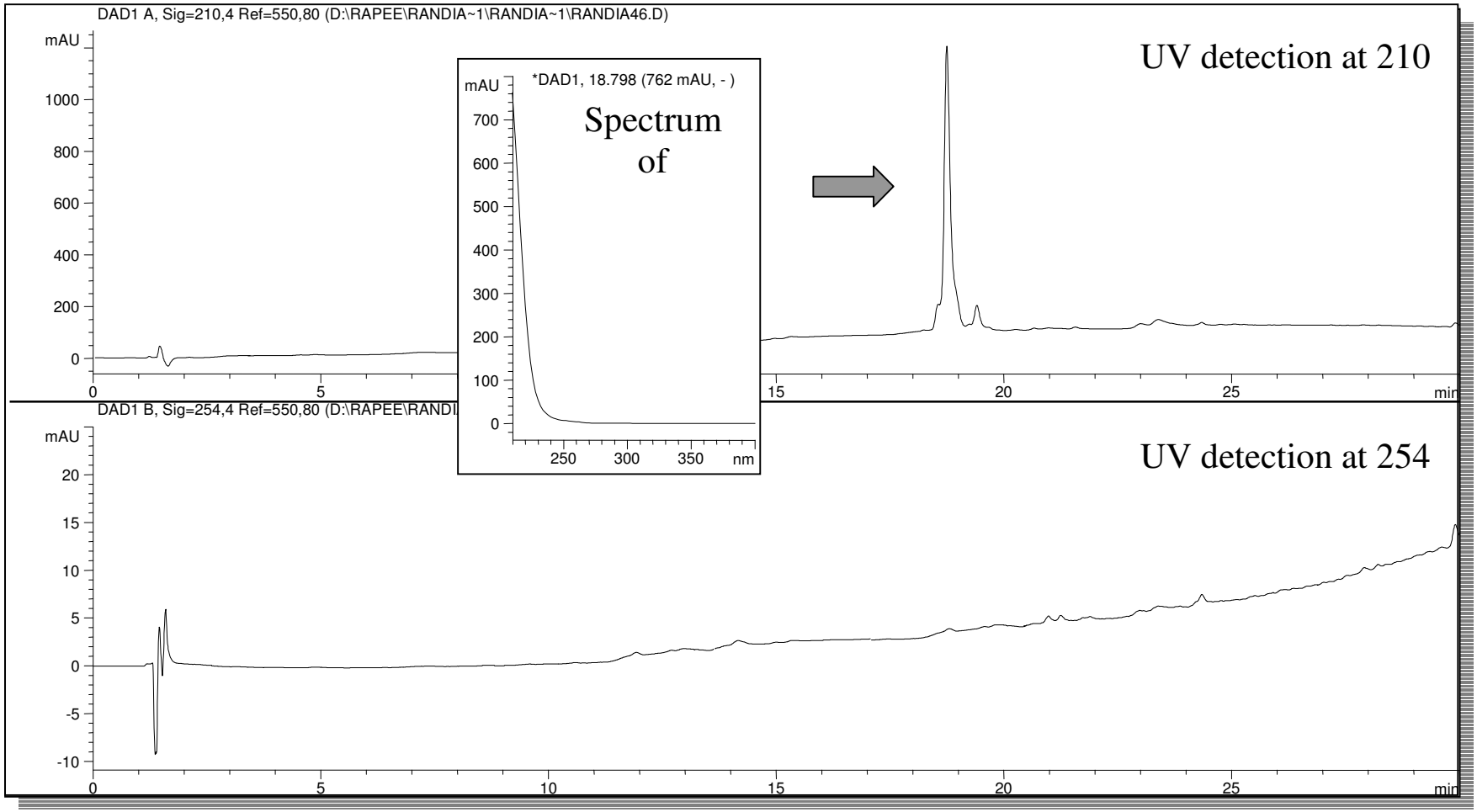

Figure 56 Representative HPLC chromatogram under the UV detection at 210 and 254 nm, and the spectrum of **compound 11,**